DESIGN AND TESTING OF A STRAW COLLECTION DEVICE FOR A RICE COMBINE HARVESTER
/
基于水稻联合收获机的秸秆收集装置设计与试验

Yanru BI, Gang WANG*, Zhuohuai GUAN, Yao YANG, Tao JIANG, Min ZHANG*
Nanjing Institute of Agricultural Mechanization, Ministry of Agriculture and Rural Affairs, Nanjing, 210014, China
Tel: +86.15366092917; E-mail: zhm0912@126.com
DOI: https://doi.org/10.35633/inmateh-78-22

Keywords: *rice straw, combine harvester, crushing, throwing, non-falling straw collection*

ABSTRACT
To address the limitations of current rice straw collection methods in China—where straw left in the field for subsequent collection is prone to soil contamination and significant losses, while non-falling harvesting combined with simultaneous baling results in low bale density and reduced harvesting efficiency—a device for simultaneous crushing and spraying of rice straw during harvesting was designed. The device integrates harvesting, straw crushing, spraying, and a vehicle-mounted baling system. Key structural parameters were determined based on the feed rate of the rice combine harvester. Four performance indicators were defined to evaluate straw crushing quality, spraying performance, and straw loss: crushing rate, straw spray mass flow rate, straw spray range, and leakage ratio. To validate the performance of the proposed device, field experiments were conducted during the rice harvesting season in Anhui Province, China, using both conventional and brittle rice varieties. Straw samples were collected before and after crushing, and the crushing rate and segment length distribution uniformity were measured. The experimental results showed that, at normal harvesting speeds, the crushing rate of Yong you 4901 reached 74.75%, while that of Ke Cui Geng No. 1 reached 96.97%, both satisfying the silage feed cutting length requirement of ≤10mm. The straw spray mass flow rate reached 5.30 kg/s, meeting the design requirement of ≥1.67 kg/s. The average spreading width was 2.92 m, with a maximum spray distance of 7.71 m, meeting the long-range spray design specification. Straw leakage accounted for 10.26%, indicating a relatively minor level of material loss. These results demonstrate that the proposed rice straw crushing and spraying device exhibits excellent crushing performance and long-range, concentrated spraying capability without adversely affecting normal rice harvesting efficiency. This study provides a useful reference for the design of efficient and low-cost rice straw collection equipment.

摘要
针对目前中国水稻秸秆田间落地再捡拾收集方式易混入土块、损耗大，不落地收获同步打捆收集捆扎密度低且影响收获作业效率等问题，基于联合收获+粉碎抛送+车载装箱模式，设计了一种水稻收获秸秆同步粉碎抛送装置。根据水稻收割机的喂入量确定了该装置的关键结构参数，定义了秸秆粉碎率、秸秆抛送量、秸秆抛洒范围、秸秆漏洒占比四个指标来评价该装置的秸秆粉碎质量、抛送性能并量化秸秆漏洒程度。为验证该装置的性能，在中国安徽省水稻收获期间分别选择常规和脆性两种水稻品种进行了田间试验，采集粉碎前后的秸秆样本，并测量秸秆粉碎率、秸秆长度分布均匀性，测量结果表明：正常机收作业速度下，甬优 4901 水稻秸秆粉碎合格率为 74.75%，科脆梗一号脆杆水稻粉碎合格率为 96.97%，均满足青贮饲料切段长度≤10mm 的要求；秸秆抛送量达 5.30kg/s，达到设计值不小于 1.67kg/s 的要求; 抛洒范围幅宽平均 2.92m，极限抛送距离 7.71m，满足远距抛送的设计要求;秸秆漏洒占比为 10.26%，秸秆漏洒较小。研究结果表明，设计的水稻收获秸秆同步粉碎抛送装置，在不影响正常水稻收获作业效率下，具有良好的粉碎性能和远距集中抛送能力，该研究可为水稻秸秆的高效低成本收集装备设计提供参考。

INTRODUCTION
Rice is China's largest grain crop, with a planting area of 434 million mu in 2023, accounting for 24.33% of the total grain planting area, and a production of 207 million tonnes. The resulting rice straw amounts to 230 million tonnes (*Xi et al., 2023*). Currently, straw utilisation primarily involves returning it to the fields or burning it, with only 18.6% being used for feed (*Yi et al., 2024*).

However, China imported 13.0937 million tonnes of feed in the same year, making the feed utilisation of straw crucial for reducing reliance on imports (*Zhixiong et al., 2021*). Rice straw used for silage has enormous economic benefits (*Ahmed et al., 2023*). The primary bottleneck constraining its feed utilisation is the lack of technology in the collection and pre-processing stages (*Weilin et al., 2023*).

The prevailing rice straw collection methods in China are primarily categorised into two approaches: ground-level gathering and non-falling baling collection. When straw is left on the ground, soil clods readily contaminate it during collection, necessitating additional soil-removal equipment (*Wang et al., 2021*) . This introduces redundant steps, high rates of missed straw, and significant losses. Chinese grain harvester companies and institutions such as Starlight, Aihe, and Zhonglian have also developed equipment for simultaneous rice harvesting and straw collection and baling (*Jianwei et al., 2022*). However, some of this equipment has issues in actual use, including low harvesting efficiency, high failure rates, and bale density that does not meet silage requirements (*Jiao et al., 2025*). Additionally, long-distance storage and transportation of rice straw is costly (*Yufeng et al., 2022*). If bales packed in the field contain impurities or have insufficient density, they need to be unpacked and re-compacted at the processing plant (*Larsen & Møller, 2024*), wasting manpower and making it hard to promote existing machinery.

Internationally, countries like the United States and Japan have established an integrated operational model of 'combined harvesting, crushing and conveying, and vehicle-mounted collection' (*Valge et al., 2021*). For example, John Deere's silage harvester achieves on-site straw processing through an integrated crushing and conveying device. However, such equipment is limited in its promotion in China's rice-growing regions due to its high cost and limited applicability to tall-stemmed crops.

Beyond commercial equipment, significant academic research focuses on optimizing the core processes involved in harvest and separation, which are foundational to any subsequent straw handling. For instance, studies on axial-flow threshing apparatus have identified optimal regimes for threshing and separation that balance grain loss and straw fragmentation, directly impacting the quality and quantity of straw available for collection (*Vlăduț et al., 2023*). Furthermore, research into the vibration characteristics of combine harvesters is crucial, as excessive vibration not only affects operator comfort and safety (*Marin et al., 2024*) but can also influence the consistency of material flow into auxiliary devices like straw processors, and complicate the identification of vibration sources for targeted improvement (*Cârdei et al., 2025*). These studies underscore the importance of a systemic approach that considers the harvester as a whole when integrating additional functional modules like straw collectors.

Therefore, achieving non-falling collection of rice straw in the field can enhance straw quality and reduce losses. This holds significant importance for on-site silage processing of rice straw in the field and subsequent industrial feed processing (*Michał et al., 2023*). This paper proposes a technical solution for long-distance, non-falling straw spray to collection vehicles during rice harvesting, tailored to China's harvesting requirements and production characteristics (*Andrey & Vladimir, 2021*). By integrating a straw crushing and long-distance spray unit to the rear of a full-feed combine harvester, facilitates efficient straw collection without compromising harvesting efficiency. This approach provides a reference for designing high-efficiency, low-cost equipment for rice straw collection.

MATERIALS AND METHODS

➢ *STRUCTURE AND WORKING PRINCIPLE*

The straw crushing and conveying device adopts a modular design, integrating a deflector housing, a crushing unit (including moving knives and fixed knives), a feed auger with spray blades and a throwing cylinder. Power is transmitted from the harvester to each component via a belt drive system. The crushing unit feeds the straw into the deflector housing for crushing. The feed auger conveys the shredded straw to the left toward the spray blades, where it is accelerated by the fan and sprayed through the throwing cylinder, with the spray position and angle adjusted as needed. The structure is shown in Figure 1.

During rice harvesting operations, the crop enters the threshing and cleaning system. During the separation process in the cleaning system, some straw is directly sprayed from the threshing drum outlet, while the remainder is sprayed from the rear of the vibrating screen (*Tao et al., 2025*). The harvester's power is transmitted through the transmission system to the knife roller shaft of the crushing device. The moving knives on the knife roller throw the straw sprayed from the threshing and cleaning system into the deflector housing. Under the combined tearing and cutting action of the moving knives and fixed knives, the straw is crushed into small segments.

Utilising rotational centrifugal force, the straw slides along the deflector housing into the feed auger. The feed auger conveys the crushed straw to one end equipped with spray blades. As the auger rotates, the throwing blades create an airflow field within the feed chamber, assisting in accelerating straw spraying.

The straw then ejected through the spray port along the upper throwing cylinder. By adjusting the deflector plates at the spray port, the spray distance of the straw can be controlled, facilitating collection by the following vehicle.

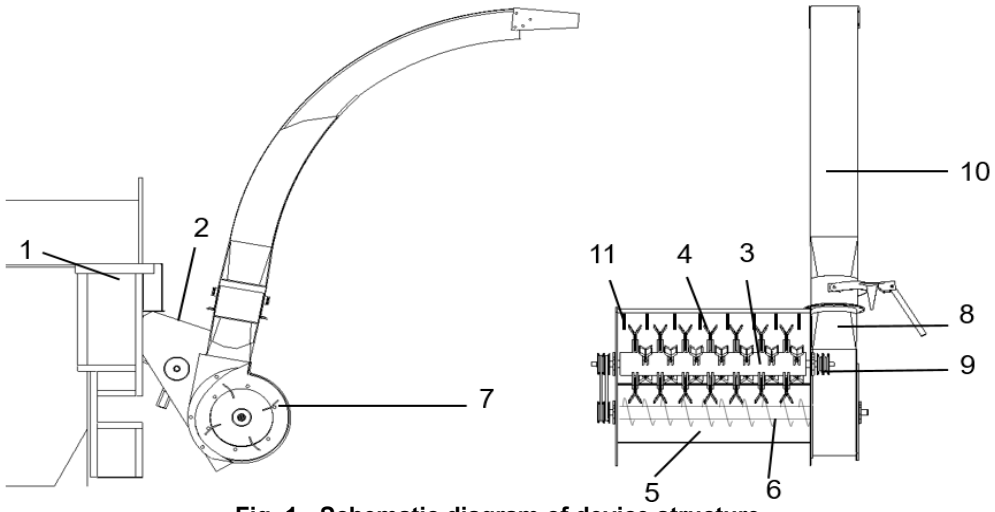

Fig. 1 - Schematic diagram of device structure

1. Harvester rear mounting frame; 2. Deflector housing; 3. Crushing knife roller; 4. Moving knife; 5. Auger housing; 6. Feed auger; 7. Throwing blade; 8. Drive belt pulley; 9. Lower throwing cylinder; 10. Upper throwing cylinder; 11. Fixed knife

➢ *MAIN TECHNICAL PARAMETERS*

To meet the requirements of combine harvester operation and material reception, the technical parameters of the device were determined, as shown in Table 1.

Table 1

Technical parameters of the device

Parameters	Numerical value
Length × Width × Height (mm×mm×mm)	1605×885×2478
Working width (mm)	725
Number of crushing blades	28
Number of fixed knife rows	3
Blade speed(rpm)	3000
Number of blades	4
Design feed rate (kg/s)	3.18
Knife roller speed (rpm)	3000
Conveying rate of screw conveyor (kg/s)	5.455

➢ *PARAMETER ANALYSIS AND STRUCTURAL DESIGN*

Straw crushing system. The straw crushing system primarily consists of fixed knives, moving knives, knife roller, left and right side plates, and a housing. During rice harvesting operations, the straw discharged from the threshing and cleaning system first enters the crushing system for crushing. The primary design parameters of the device were determined by balancing the harvesting efficiency of the combine harvester with the requirements for cutting length in silage pre-treatment (*Liu et al., 2023*).

(1) Straw feed rate

The primary design requirement of the proposed device is that it does not adversely affect the harvesting efficiency of the rice combine harvester. Therefore, the feed rate of the device is determined based on the feed rate of the combine harvester.

The calculation formula is:

$$Q = \frac{q}{1+\beta} \quad (1)$$

In the formula, Q is the feed input (kg/s); q is the harvester feed input (kg/s); β is the grain-to-straw ratio. The straw-to-grain ratio denotes the proportion of above-ground crop stalk yield to the yield of the crop's primary product. It serves as a crucial indicator for evaluating crop output efficiency, also termed the ratio of crop by-products to main products.

It is expressed by the formula:

$$\beta = \frac{W_s}{W_p} \quad (2)$$

where W_s represents the crop stalk yield; W_p denotes the crop primary product yield.

Extensive rice cultivation trials and production practices indicate that the straw-to-grain ratio for early, mid-season, and late rice varieties generally follows this relationship: early rice < mid-season rice < late rice. The typical range for rice straw-to-grain ratios is between 0.9 and 1.5. Based on actual cultivation conditions in the trial region, β is set at 1.1. q is taken as 3.5 kg/s, yielding a calculated feed input rate Q of 1.67 kg/s.

(2) Crushing knife

This design adopts a reverse crushing method, which requires the cutting knife to have a certain degree of picking performance (*Kun & Yuepeng, 2022; Yue et al., 2021*). Saw-toothed swing knives have good picking performance and tearing effects (*Jiang et al., 2021*), so saw-toothed swing knives and multiple sets of saw-toothed fixed knives are initially selected for the moving and fixed knife combination. The structure and assembly dimensions are as shown in the Figure 2. The arrangement of the crushing knife rollers significantly influences the overall vibration of the machine and the stress on the bearings at both ends. A symmetrical arrangement facilitates easier balancing. A total of 28 sets of moving knives and 15 sets of fixed knives are arranged. The rotational radius of the knife rollers is 205 mm, with a minimum clearance of 22 mm from the housing.

Based on the design working width, the final mating dimensions between moving and stationary blades were determined: D_1 = 19 mm, D_2 = 8 mm, and D_3 = 56 mm. Testing confirmed no interference occurs between moving and stationary blades.

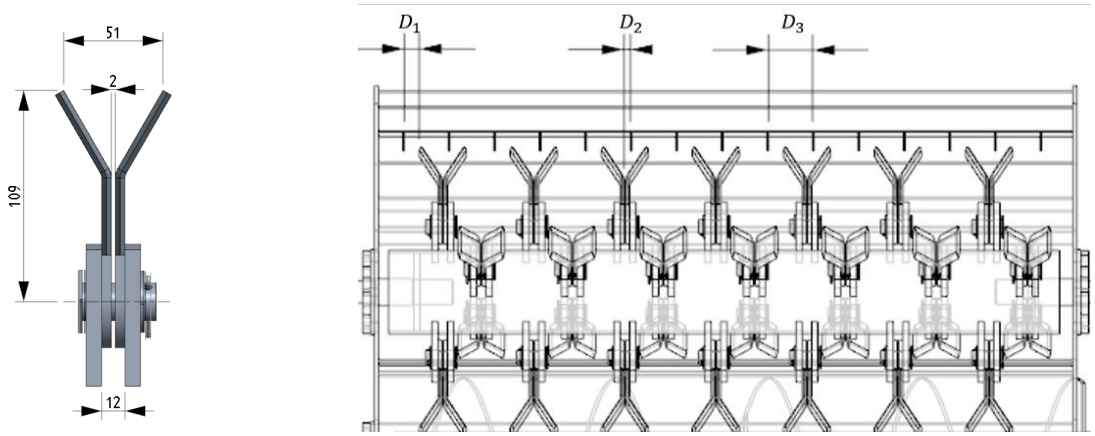

Fig. 2 - Crushing Blade Structure and Key Dimensions

(3) Crushing knife roller speed

The number of moving knives is related to power consumption. To improve the quality of crushing, the layout of the moving blades is determined based on the width of the harvester's straw spray port. The moving knives are arranged in a circular pattern (*Li et al., 2024*), with 28 sets of moving blades divided into four rows, each row containing seven sets of moving knives. The four rows are evenly distributed around the circumference of the knife roller, and adjacent rows of moving knives are arranged in an offset pattern to ensure uniform crushing of the straw.

The speed of the knife roller is related to the number of moving knives, and the calculation formula is (*Qiang et al., 2024*):

$$n = \frac{60000v}{z\,Lp} \quad (3)$$

In the formula, n is the rotational speed of the knife roller (r/min); L_p is the chopped length of straw (mm); v is the discharge speed of straw (m/s); z is the number of moving blades on the knife roller.

The mass of straw that the crushing roller can cut and process per unit of time must be greater than the mass of straw discharged from the rear of the harvester per unit of time. The density of the straw remains constant during this process, so it is only necessary to compare the volume of straw discharged per unit of time with the volume of straw that the crushing roller can cut and convey per unit of time.

The volume of straw that the crushing roller can shred and convey per unit time, V_1 (m3/s), can be calculated using the following formula:

$$V_1 = \frac{n}{60}[\pi h(D^2 - d^2) - zabc] \quad (4)$$

In the formula, n is the rotational speed of the knife roller (r/min), based on simulation tests, taken 2500 r/min; h is the length of the knife roller (mm), taken 855 mm; D is the diameter of the circular trajectory of the moving knife tip (mm), taken 410 mm; d is the diameter of the knife roller (mm) , taken 115 mm; z is the number of moving knives, taken 28; a is the length of the moving knife (mm) , taken 109 mm; b is the width of the moving knife (mm), taken 48 mm; c is the thickness of the moving knife (mm), taken 5 mm.

The volume V_2(m³/s) of straw discharged from the harvester per unit time can be calculated using the following formula:

$$V_2 = v(S_1 + S_2) \tag{5}$$

In the formula, v is the discharge velocity of straw (m/s), measured as 10 m/s; S_1 is the area of the straw discharge opening of the threshing drum (m²), with a measured diameter of 314 mm. As the discharge opening occupies the lower half of the drum, the calculated area is 0.154795 m²; S_2 is the area of the cleaning discharge opening (m²), measured as 0.029925 m².

After calculation, V_1 = 17.386 m³, V_2 = 1.8472 m³, where $V_1 > V_2$. The crushing section can satisfy the straw feed rate of the combine harvester.

(4) Straw conveyor system

After being crushed by the crushing roller, the straw is conveyed along the housing into the screw conveyor. During this process, the straw has an initial velocity and is subjected to its own weight and friction with the housing. The screw conveyor must be able to handle the majority of the crushed straw (*Ma et al., 2024*). Theoretically, whether in the crushing section or the conveying section, the feed rate represents the maximum mass of straw that can be received per unit of time. Therefore, the conveying rate of the screw conveyor is designed based on the feed rate as the standard.

The formula for calculating the conveying rate Q of screw conveyor is (*Qiang et al., 2024*):

$$Q = \frac{\pi}{24}[(D - 2\lambda)^2 - d^2]\psi tn\gamma C \times 10^{-10} \tag{6}$$

In the formula, D represents the outer diameter of the conveyor blade (mm); d represents the inner diameter of the conveyor blade (mm); t represents the pitch of the conveyor blade (mm); λ is the clearance between the conveyor blades and the housing (mm); n is the conveyor speed (rpm); ψ is the filling coefficient when conveying rice straw, typically taken as 0.3 to 0.4; γ is the mass per unit volume of rice straw (kg/m³); C is the inclined conveying coefficient of the conveyor.

After calculation, the conveying rate of the screw conveyor was found to be 5.455 kg/s, which is greater than the feed rate of 3.18 kg/s required by the design.

(5) Straw throwing system

During operation, the gap between the throwing blades and the screw conveyor blades prevents blockages from forming where the two interact. The straw flow is pushed towards the throwing blade end by the conveying action of the screw conveyor (*Gu et al., 2022*).

In the first stage of straw throwing, when the throwing blades rotate, the straw is subjected to gravity, centrifugal force, G-force, blade normal reaction force, and friction force. When the blades move to a certain position, the straw separates from the blades and enters the upper throwing cylinder (*Bulgakov et al., 2023*).

The diameter of the baffle plate is determined based on the diameter of the spiral blades and is set to 285 mm. The installation methods for the flat blades include forward-inclined and backward-inclined configurations. Among these, forward-inclined blades may experience a phenomenon where straw cannot be ejected at certain rotational speed ranges, resulting in significant limitations. Therefore, the backward-inclined installation method is selected for the blades. The minimum ejection rotational speed for backward-inclined blades is ω_{min}. According to the research findings, the formula for calculating the minimum rotational speed is (*Mei et al., 2021*):

$$\omega_{min} > \sqrt{\frac{g}{r_0 \sin\varphi + l_1 \cos\varphi}} \tag{7}$$

$$f = \tan\varphi \tag{8}$$

In the formula, φ is the friction angle of the straw, r_0 is the deviation of the particle on the blade, and l_1 is the coordinate of the initial position of the particle. After calculation, the designed rotational speed of 3000r/min is greater than ω_{min}, which can throw the straw into the upper throwing cylinder.

When the straw particle reaches the blade edge, the following relationship holds:

$$l = R\cos\delta_1 \tag{9}$$

At this point, the throw angle φ_L is:

$$\varphi_L = \sqrt{\frac{2(R\cos\delta_1 - l_2)}{fr_0 + l_2}} \quad (10)$$

In the equation, δ_1 is the installation angle of the backward-curved blade, l_2 is the coordinate at the edge of the blade, under the condition of:

$$\omega^2(fr_0 + l) \geq \frac{g}{\cos\varphi} \quad (11)$$

The throw angle φ_L is independent of the rotational speed and initial phase, and is only related to the friction coefficient and structural parameters. Therefore, they can be used to estimate the magnitude of φ_L during preliminary design and used as qualitative design.

In the second stage of straw conveying, the straw enters into the upper throwing cylinder, subject to the friction of airflow and pipe wall, and is thrown upwards to touch the cylinder wall.

The upper and lower area of the throwing cylinder is determined by the area factor (*Qiang et al., 2024*).

$$m_{tv} = \frac{s_1}{s_2} \quad (12)$$

where m_{tv} is the area factor, usually taken as 0.55~0.65, s_1 is the area of the upper throwing cylinder, s_2 is the area of the lower throwing cylinder. Changes in pipe area will affect changes in airflow (*Khan et al., 2025*).

The third stage of straw conveying, after the acceleration of the first two stages, the straw collides with the wall of the upper throwing cylinder and loses part of the kinetic energy and then sprays out of the spray port of the upper throwing cylinder.

- ***SIMULATION TEST DESIGN***

Using the discrete element method (DEM), simulation analysis was conducted and compared with actual operating conditions to validate the accuracy of the simulation. The performance of the device in throwing straw was analyzed to determine the optimal combination of structural parameters. Simplified modeling of the device was performed using the 3D modeling software CREO and imported into the EDEM software. A straw model with varying lengths and thicknesses, as shown in Figure 3, was established to simulate actual operating conditions. During simulation, the crushing roller and auger-maintained rotation. Statistical zones for strip-like spillage and ejection were established within the device, as shown in Figure 4. The Hertz-Mindlin contact model was selected for contact modeling. Based on the team's preliminary work, the model contact parameters are as shown in Table 2.

Based on the team's preliminary work, it was determined that when straw exits the rear of the threshing cylinder, its distribution ratio on either side of the cylinder is 4:3. The straw feed rate at the rear of the threshing cylinder was determined to be 2.5 kg/s, while the feed rate at the straw discharge outlet was 1.25 kg/s. Within the simulation model, the straw ejection velocity was set at 10 m/s. According to the actual spatial configuration of the threshing drum, particle factories generating straw were positioned on the left and right sides of the cylinder, with generation rates of 1.43 kg/s and 1.07 kg/s respectively. A rectangular particle factory measuring 35 mm × 855 mm was positioned at the actual location of the straw discharge outlet, with a straw generation rate of 1.25 kg/s and an ejection velocity of 10 m/s.

Fig. 3 - Straw Modeling

Table 2

Simulation Parameters

Parameters	Numerical Value
Straw Poisson Ratio	0.41
Straw density /kg·m^3	241
Straw shear modulus /Pa	9.1× 10^6
Steel's ratio	0.3
Steel density /kg·m^3	7400
Steel shear modulus /Pa	7.9× 10^{10}
Straw-Straw Recovery Coefficient	0.3
Straw - Static Friction Coefficient of Straw	0.3
Straw-Straw Rolling Friction Coefficient	0.01
Straw-Steel Recovery Coefficient	0.3
Straw - Static Friction Coefficient	0.3
Straw-Steel Rolling Friction Coefficient	0.01

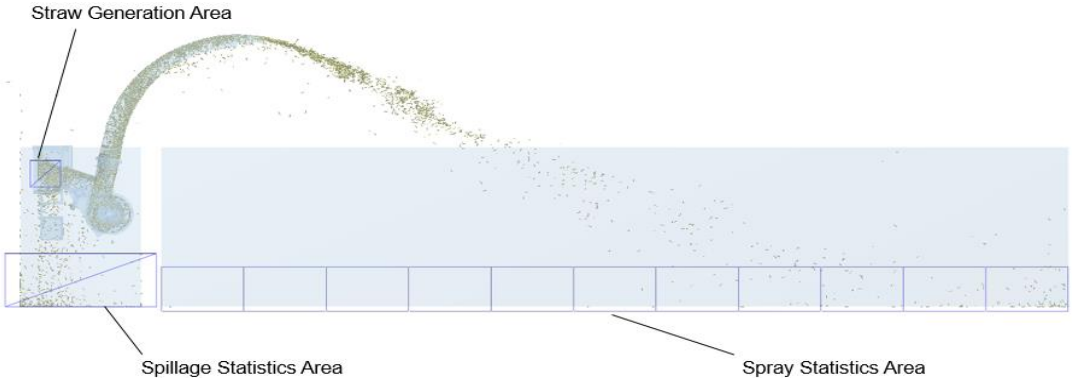

Fig. 4 - Device Simulation Model

➢ ***VERIFICATION OF SIMULATION MODEL***

In the discrete element simulation model, the crushing roller speed was set to 3000 r/min, the feed rate to 2.5 kg/s, and the auger speed to 3000 r/min. The rotational directions of the crushing roller and the auger were aligned. The straw generation rate at the rear of the threshing drum was set at 2.5 kg/s, while the straw generation rate at the cleaning and straw discharge outlet was set to 1.25 kg/s. The simulation results indicated a spillage mass of 0.38 kg and an ejection mass of 1.74 kg. Based on the defined spillage evaluation metrics, the calculated spillage rate was 18%. Measurement of the straw ejection distance showed a maximum projection distance of 6.26 m.

To validate the simulation model's accuracy, a field trial apparatus was designed and prototyped according to the device's structural dimensions, as depicted in Figure 5.

On 16 October 2024, field trials for rice straw crushing and ejection were conducted in Mingguang, Anhui Province. The test apparatus operated with a crushing roller speed of 3000 r/min, feed rate of 2.5 kg/s, and auger speed of 3000 r/min. Field measurements recorded a spillage rate of 12.66% and a spray distance of 6.95 meters. The absolute error for spillage rate was 5.43%, with a relative error of 42.18%. The relative error for spray distance was 10.07%. Comparison of simulation results with field tests revealed minimal absolute error, confirming the suitability of the established discrete element model for subsequent structural parameter optimization.

Fig. 5 - Field verification test

➢ ***EXPERIMENTAL DESIGN FOR PARAMETER OPTIMISATION***

Based on a discrete element model constructed and validated for simulation accuracy, multiple single-factor simulations were conducted using three key structural and operational parameters - straw feed rate, crushing roller speed, and auger speed - as experimental factors, with spray distance as the response indicator. This comprehensive evaluation of each factor's impact on device performance preliminarily determined the optimal feed rate range to be 2 kg/s to 3 kg/s, crushing roller speed of 2000–3000 r/min, and auger speed of 2000–3000 r/min. The experimental factor levels are shown in Table 3. To further optimize the structural parameters, a three-factor, three-level Box-Behnken experimental design was employed to investigate the influence of these factors on the device's throwing distance. A comprehensive evaluation method was used to select the optimal parameter combination.

Table 3

Levels of Factors in the Three-Factor, Three-Level Box-Behnken Experiment

level	Feed rate (kg/s)	Crushing roller speed (r/min)	Auger speed (r/min)
-1	2	2000	2000
0	2.5	2500	2500
1	3	3000	3000

RESULTS AND ANALYSIS

➢ *RESULTS AND ANALYSIS OF THE BOX-BEHNKEN EXPERIMENT*

Following the Box-Behnken experimental design, this study conducted a three-factor, three-level response surface experiment, testing a total of 17 experimental combinations. The experimental results are presented in Table 4.

Table 4

Results of the Three-Factor, Three-Level Box-Behnken Experiment

	Test Factors and Levels			Test Indicators
	A Feed rate (kg/s)	B Crushing roller speed (r/min)	C Auger speed (r/min)	Y (m)
Test No.	-1	-1	0	5.75
	1	-1	0	5.55
	-1	1	0	5.42
	1	1	0	6.12
	-1	0	-1	6.12
	1	0	-1	6.56
	-1	0	1	7.25
	1	0	1	7.5
	0	-1	-1	5.5
	0	1	-1	5.95
	0	-1	1	6.95
	0	1	1	6.76
	0	0	0	6.56
	0	0	0	6.49
	0	0	0	6.43
	0	0	0	6.55
	0	0	0	6.52

This experiment employed Design-Expert 13 software to perform regression fitting analysis on the test results in Table 4, yielding the regression equations for the coded values of each factor with respect to throwing distance:

$$Y = 6.51 + 0.1488A + 0.0625B + 0.413C + 0.2250AB - 0.0475AC - 0.1600BC - 0.1163A^2 - 0.6838B^2 + 0.4638C^2$$

After processing with Design-Expert software, the results of the variance analysis for throwing distance are shown in Table 3. As indicated by the variance analysis results in Table 3, the models for power consumption and straw crushing rate are significant ($p<0.05$). For the objective function, factors C, AB, B^2, and C^2 are highly significant. The order of significance for each factor affecting throwing distance, from highest to lowest, is: auger speed, crushing roller speed, and feed rate. The analysis of variance table for the throwing distance test is shown in Table 5.

Table 5

Analysis of Variance Table for Throwing Distance Test

Source	df	SS	MS	F	P
Model	9	5.68	0.6308	219.94	< 0.0001
A	1	0.1770	0.1770	61.72	0.0001
B	1	0.0313	0.0313	10.90	0.0131
C	1	2.34	2.34	817.20	< 0.0001
AB	1	0.2025	0.2025	70.61	< 0.0001
AC	1	0.0090	0.0090	3.15	0.1193
BC	1	0.1024	0.1024	35.71	0.0006
A2	1	0.0569	0.0569	19.84	0.0030
B2	1	1.97	1.97	686.39	< 0.0001
C2	1	0.9055	0.9055	315.75	< 0.0001
Residual	7	0.0201	0.0029		
Lack of Fit	3	0.0091	0.0030	1.10	0.4462
Pure Error	4	0.0110	0.0028		
Cor Total	16	5.70			
R2	0.9965				

➢ ***RESPONSE SURFACE METHODOLOGY ANALYSIS***

The primary factors affecting throwing distance, in order of significance, are auger speed, crushing roller speed, and feed rate. Significant ($P<0.05$) interactions exist between feed rate and crushing roller speed, as well as between crushing roller speed and auger speed. As shown in Fig. 6, the throwing distance first increases and then decreases with increasing crushing roller speed, reaching its maximum at 2500 r/min. As shown in Fig. 7, both feed rate and auger speed increase the throwing distance. Auger speed has a particularly significant effect, while feed rate has a relatively minor impact. The maximum throwing distance occurs at an auger speed of 3000 r/min and a feed rate of 3 kg/s. As shown in Fig. 8, the throwing distance first increases and then decreases with increasing shredder roller speed. The maximum throwing distance occurs when the auger speed reaches its peak of 3000 r/min. This is because when the shredder roller speed exceeds 2500 r/min, the straw enters the auger too rapidly, preventing the auger from adequately conveying the straw.

Using the Optimization function in Design-Expert software, an optimization analysis was conducted. Considering the actual operating conditions and processing requirements of the combine harvester, the optimized parameter combination was obtained: feed rate of 2.5 kg/s, crushing roller speed of 2500 r/min, and auger speed of 3000 r/min.

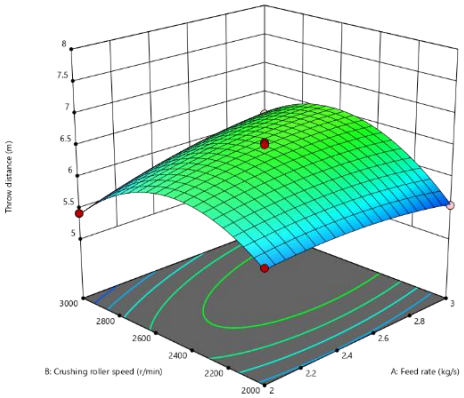

Fig. 6 - Effects of AB

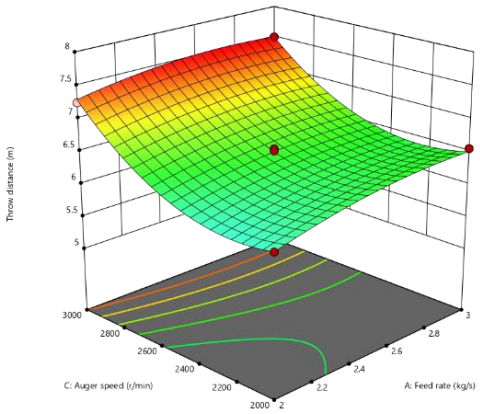

Fig. 7 - Effects of AC

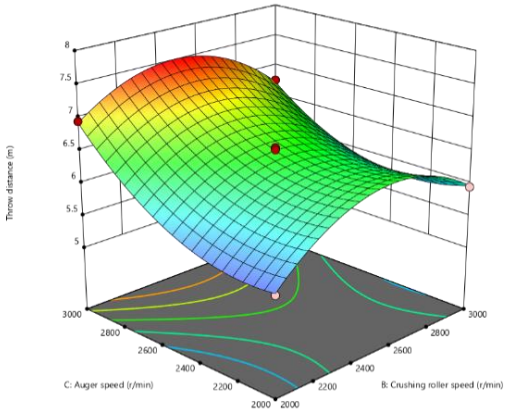

Fig. 8 - Effects of BC

➢ ***FILED TEST CONDITIONS AND METHODS***

On 16th October and 25th October 2024, a field rice harvest straw crushing and throwing test was carried out in Mingguang, Anhui Province and Lujiang, Anhui Province respectively. The average ambient temperature at the Mingguang experimental field was 20°C, and the average wind speed at a height of 1.2 m above the ground was 3 m/s and the relative air humidity was 84%. The rice variety cultivated in the Mingguang test field was *Yong you 4901*, with an average plant height of 125 cm, a straw moisture content of 66.53% and a grain yield of 616 kg per mu. The transmission ratio between the crushing knife roller and the auger drive shaft was set to 1:1. At the Lujiang experimental site, the average ambient temperature was 22°C, and the average wind speed at a height of 1.2 m above the ground was 3 m/s. The relative air humidity was 73%. The rice variety cultivated in the Lujiang test field was *Ke cui geng No. 1*, with an average plant height of 134 cm, a straw moisture content of 75.47%, and a grain yield of 704 kg per mu. The gear ratio of the crushing roller and auger drive shaft assembly was 5:6. The rotational speed range of the assembly's power take-off shaft was 0-3000 r/min, meeting the experimental requirements. During testing, the following parameters were selected following simulation optimization: a feed rate of 2.5 kg/s, a crushing roller speed of 2500 r/min, an auger speed of 3000 r/min.

The evaluation indicators for assessing the operational quality of rice straw crushing and conveying equipment primarily include the rate of crushing, straw spray mass, straw spray range, and the leakage ratio, among others. These indicators reflect the equipment's performance in terms of straw crushing and spray.

The rate of crushing is an important indicator of crushing effectiveness. According to the crushing requirements for rice straw as silage feed, a segment length of 10 mm or less is considered acceptable. The calculation formula is as follows:

$$\eta = \frac{L_2}{L_1} \tag{13}$$

where L_2 is the number of straw lengths within 10 mm in length; L_1 is the number of all straw lengths.

In addition, the straw was randomly divided into groups, and the uniformity of the straw segment lengths before and after crushing was compared and tested as an indicator of crushing quality.

First, disconnect the device from the harvester's power source and hang a piece of canvas of appropriate size behind the harvester to collect the straw discharged from the harvester. After collection is complete, reconnect the power source and repeat the collection and measurement process.

Straw spray range: This indicator includes the spray width and the limiting spray distance. After the harvester passes through the calibration measurement section, the measurement section is divided into five groups at 1-metre intervals. A tape measure is used to measure the swath width of straw in each group (grouping details are shown in Figure 9). Straw that falls is collected using a canvas suspended below the crushing system for subsequent measurement and calculation. When measuring the limiting spray distance, after the harvester passes, the straight-line distance from the far end of each group of fallen straw to the centre axis of the throwing pipeline is measured, and the average value is taken as the limiting spray distance.

Leakage ratio: Test the mass m_2 of straw falling under normal operating conditions and the ratio μ of the falling mass to the throwing mass m_1 as indicators for evaluating the picking capacity of the crushing device. The calculation formula is as follows:

$$\mu = \frac{m_2}{m_1} \tag{14}$$

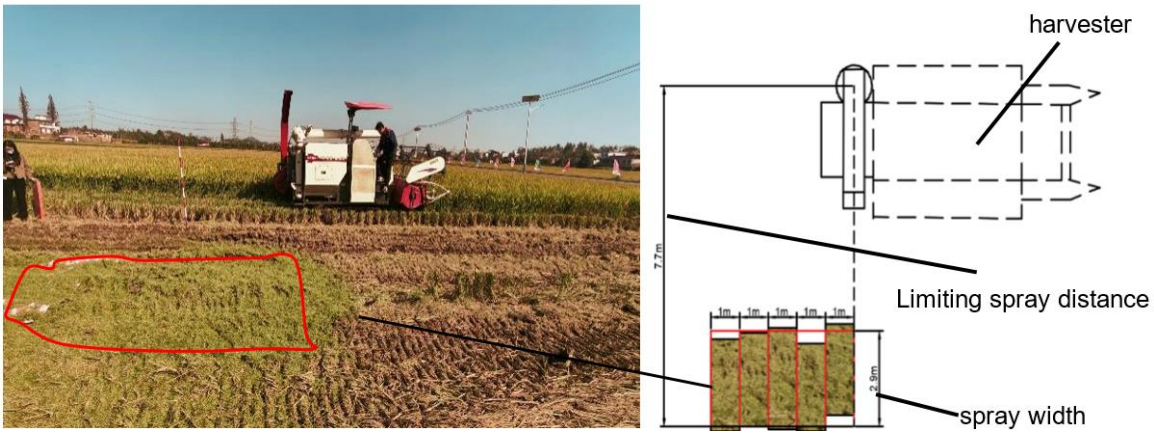

Fig. 9 - Schematic diagram of straw fallout range measurement

➢ *FILED TEST RESULTS AND ANALYSIS*

To more clearly illustrate the changes in straw segment length before and after crushing, a scatter plot of the segment length distribution was generated (Fig. 10), and a preliminary statistical analysis of the collected segment length data was conducted, with the results presented in Table 6. In the harvesting trial of Yong you 4901, the straw segment length before crushing was generally greater than 20 mm, whereas after crushing, most segments were shorter than 10 mm, yielding a crushing rate of 74.75%, which meets the silage feed requirement for straw segment length. In the harvesting trial of Ke cui geng No.1, the straw segment length before crushing was mainly around 10 mm, and after crushing, most segments were also below 10 mm, resulting in a crushing rate of 96.97%. From a statistical perspective, the mean value, variance, and standard deviation of the straw segment lengths after crushing were all significantly lower than those before crushing, indicating that the crushing process substantially improved the uniformity of the chopped straw segments.

Table 6

Statistical values for sample segment lengths before and after crushing

Eigenvalues	October 16th, Harvest of Yong you 4901		October 25th, Harvest of Ke cui geng No. 1	
	Before crushing	After crushing	Before crushing	After crushing
Maximum (mm)	50	43	12	9
Minimum (mm)	7	1.5	3	1
Average deviation	10.25	6.01	1.83	1.07
Variance	142.28	67.92	5.38	2.22
Average	27.57	10.44	7.03	3.27

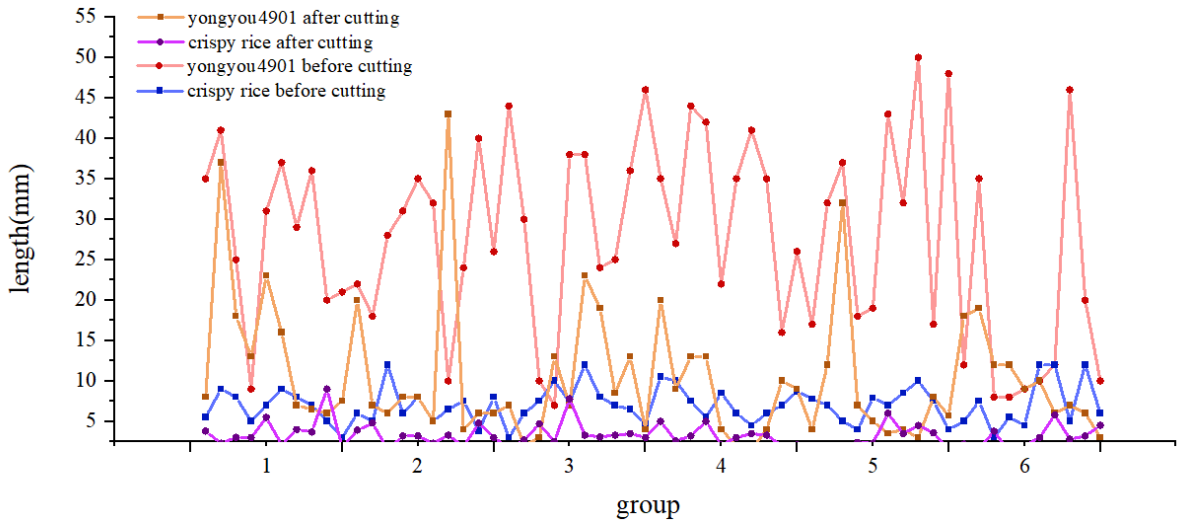

Fig. 10 - Comparison of sample segment lengths before and after crushing

The test results indicate that the average collected straw mass was 10.60 kg, with a leakage ratio of 10.26%. The average spray width was 2.92 m, and the limiting spray distance reached 7.71 m. These indicators reflect the spatial coverage and projection capability of the straw distribution. The straw spray mass flow rate reached 5.30 kg/s, exceeding the designed requirement of 1.67 kg/s, thereby satisfying the design specifications. After parameter optimization, the leakage ratio and spray distance were improved by 18.96% and 10.79%, respectively.

Table 7

Task Metrics

Group	Quality of reception (kg)	Distance travelled (m)	Leakage ratio (%)	Spray width (m)	Limiting spray distance (m)
1	11.21	5	11.36	3.15	7.32
2	9.98	5	9.23	2.84	7.14
3	10.61	5	10.19	2.92	7.71

CONCLUSIONS

To promote efficient and high-quality utilization of rice straw, a simultaneous rice straw crushing and throwing device for combine harvesting was designed. The device enables long-distance straw throwing during rice harvesting, thereby creating favorable conditions for rapid straw collection, storage, and transportation required for efficient and clean silage production. Through theoretical analysis of the key components, the main structural parameters were determined, and the fundamental operating requirements, such as straw feed rate, screw conveying capacity, and throwing blade rotational speed, were established.

A discrete element simulation model was established and validated for accuracy. Using the feed rate, crushing roller speed, and auger speed as optimization factors, a three-factor, three-level response surface analysis was performed with Design-Expert software. The results indicated that the influence of each factor on the spray distance and leakage ratio, in descending order of significance, was auger speed, crushing roller speed, and feed rate. The optimal parameter combination for the apparatus was determined as a feed rate of 2.5 kg/s, a crushing roller speed of 2500 r/min, and an auger speed of 3000 r/min.

Field trial results showed that the straw leakage ratio was 10.26%, while the straw spreading range met the design specifications, with a limiting spray distance of 7.71 m and a spreading width of 2.92 m. The straw crushing rates for the two rice varieties reached 96.97% and 74.75%, respectively, and the straw spray mass flow rate reached 5.30 kg/s, exceeding the designed straw feed rate of 1.67 kg/s. After optimization of the device parameters, the leakage ratio and spray distance were improved by 18.96% and 10.79%, respectively. These performance metrics demonstrate that the developed machinery achieves high efficiency in straw collection and processing under field operating conditions, meeting the relevant technical standards and the practical requirements for silage production.

ACKNOWLEDGEMENT

We acknowledge the Chinese Academy of Agricultural Sciences (CAAS) Institute-level Basic Science Research Operating Expenses Project (Project No. S202403, Key Technology Research and Device Trial Production for Rice Grain and Grass Harvesting), Chinese Academy of Agricultural Sciences (CAAS) Innovation Project, Hunan Provincial Intelligent Agricultural Machinery and Equipment Innovation and R&D Project (Xiangcai Agricultural Instruction [2023] No. 60) to carry out this work.

REFERENCES

[1] Alengebawy, Ahmed & Ran, Yi & Ghimire, Nirmal & Osman, Ahmed & Ai, Ping (2023). Rice straw for energy and value-added products in China: a review. *Environmental chemistry letters*, Vol. 21(5), pp. 31-32.

[2] Andrey, B., & Vladimir, V. (2021). Rationale for vehicle parameters for the transportation of straw and hay. *BIO Web of Conferences*, Vol. 37.

[3] Bulgakov, V., Holovach, I., Ivanovs, S., Aboltins, A., Trokhaniak, O., Ihnatiev, Y., & Ruzhylo, M. (2023). Theory of movement of the sugar beet tops in loading mechanism, taking into account the influence of the air flow. *Applied Sciences*, 13(20).

[4] Cârdei, P., Vlăduț, N.-V., Biriș, S.-Ș., Oncescu, T.-A., Ungureanu, N., Atanasov, A. Z., . . . Isticioaia, S. (2025). Identification of Vibration Source Influence Intensity in Combine Harvesters Using Multivariate Regression Analysis. *Applied Sciences*, 15(18), 10159.

[5] Jiang, W., Xiaoyan, W., Hongwen, L., Jin, H., Caiyun, L., & Di, L. (2021). Design and experiment of rice straw chopping device for agitation sliding cutting and tearing. *Transactions of the Chinese Society for Agricultural Machinery*, Vol. 52(10), pp. 28-40.

[6] Jianwei, F., Chao, J., Haopeng, L., Weikang, W., Guozhong, Z., Yuan, G., . . . Anwer, A. M. (2022). Research progress and prospect of mechanized harvesting technology in the first season of ratoon rice. *Agriculture,* 12(5), 620.

[7] Jiao, L., Hao, Z., Zhang, Y., Wang, Z., Zhou, H., & Fu, P. (2025). Design and test of a baling compression and net-wrapping device for self-propelled straw-harvesting and -baling machines. *Agriculture*, 15(6), 629.

[8] Khan, A., Aabid, A., Akhtar, M. N., Khan, S. A., & Baig, M. (2025). Supersonic flow control with quarter rib in a duct: An extensive CFD study. *International Journal of Thermofluids*, Vol. 26, 101060.

[9] Kun, W., & Yuepeng, S. (2022). Research progress analysis of crop stalk cutting theory and method. *Transactions of the Chinese Society for Agricultural Machinery*, Vol. 53(06), pp. 1-20.

[10] Larsen, S. U., & Møller, H. B. (2024). Baling and ensiling of wet cereal straw as combined storage and pretreatment for biogas production. *Biomass and Bioenergy*, Vol. 187, 107294.
[11] Li, W., Zhang, F., Luo, Z., Zheng, E., Pan, D., Qian, J., . . . Wang, X. (2024). Straw movement and flow field in a crushing device based on CFD-DEM coupling with flexible hollow straw model. *Biosystems Engineering*, Vol. 242, pp. 140-153.
[12] Liu, H., Li, X., Hu, J., Zhao, J., Xu, G., Dong, D., . . . Shao, T. (2023). Fermentation quality and aerobic stability evaluation of rice straw silage with different ensiling densities. *Fermentation*, 10(1).
[13] Ma, Z., Wu, Z., Li, Y., Song, Z., Yu, J., Li, Y., & Xu, L. (2024). Study of the grain particle-conveying performance of a bionic non-smooth-structure screw conveyor. *Biosystems Engineering*, Vol. 238, pp. 94-104.
[14] Marin, E., Cârdei, P., Vlăduţ, V., Biriş, S.-Ş., Ungureanu, N., Bungescu, S. T., . . . Popa, L.-D. (2024). Research on the influence of the main vibration-generating components in grain harvesters on the operator's comfort. *INMATEH – Agricultural Engineering*, Vol. 74(3), pp. 800-815.
[15] Mei, F., Zhihong, Y., Wenjie, Z., Weifeng, L., Zhenjiang, B., & Jinbao, S. (2021). Analysis and experiments of the movement process for the shreddedmaterial of disc knife chaff cutter. *Transactions of the Chinese Society of Agricultural Engineering*, Vol. 37(07), pp. 76-84.
[16] Michał, Z., Mateusz, N., Jarosław, M., Jan, S., Stanisław, L., Julia, G., . . . Roman, R. (2023). Control and measurement systems supporting the production of haylage in baler-wrapper machines. *Sensors*, Vol. 23(6), 2992.
[17] Qiang, Z., Liusuo, L., & Jinsong, Z. (2024). *NONGYE JIXIEXUE* (2 ed.): Chemical Industry Press.
[18] Tao, J., Haitong, L., Minghui, H., Min, Z., Mei, J., & Zhuohuai, G. (2025). Design and experiment of spiral interlaced threshing cylinder for combine harveste. *Transactions of the Chinese Society for Agricultural Machinery*, Vol. 56(02), pp. 314-324.
[19] Vlăduț, N.-V., Ungureanu, N., Biriş, S.-Ş., Voicea, I., Nenciu, F., Găgeanu, I., . . . Teliban, G.-C. (2023). Research on the Identification of Some Optimal Threshing and Separation Regimes in the Axial Flow Apparatus. *Agriculture*, 13(4), 838.
[20] Wang, Q., Jiang, Y., Li, L., Qin, J., & Chen, L. (2021). Performance analysis of a spring-tooth drum pickup of straw baler via coupling simulation. *International Journal of Agricultural and Biological Engineering*, Vol. 4, pp. 14.
[21] Weilin, L., Shuming, X., Tao, L., Rui, S., Yangjie, Y., & Nengmin, Z. (2023). Carbon emissions and economic cost of different collection, storage, and transportation models for crop straw off-field utilization. *Waste and Biomass Valorization*, Vol. 15(5), pp. 2989-3001.
[22] Xi, C., Xubin, Z., Wang, Z., Huanhe, W., Tiaoyao, M., & Guisheng, Z. (2023). Utilization status of rice straw and research progress of feed processing technology in China. *China Rice*, Vol. 29(02), pp. 24-27+33.
[23] Yi, Z., Zhiyu, X., Renhua, S., Yi, Y., Haojie, F., & Yinhao, X. (2024). Research progress of straw feed based on bibliometrics. *Chinese Agricultural Science Bulletin*, Vol. 40(01), pp. 102-111.
[24] Yue, L., Chaofan, G., Deyu, Y., Ningbo, H., Xirui, Z., Zihan, W., & Yuan, L. (2021). Design and experiment of banana straw crushing and returning machine with anti-wrapping device supported by flailing blade. *Transactions of the Chinese Society of Agricultural Engineering*, Vol. 37(18), pp. 11-19.
[25] Yufeng, S., Bin, Y., Yapeng, W., Zipeng, Z., Jinwei, W., Yaping, Y., & Wenlong, M. (2022). Carbon footprint analysis of straw collection, transportation, and storage system for power generation in China based on emergy evaluation. *Environmental science and pollution research international*, Vol. 29(44), pp. 66922-66934.
[26] Zhixiong, D., Ming, G., & Lei, H. (2021). The impacts of import-side changes in grain supply on China's food security. *Chinese Rural Economy*, Vol. 1, pp. 15-30.